# Evaluation of Detection Performance for Safety-Related Sensors in Low-Visibility Environments

Yasushi Sumi[iD], Bong Keun Kim, and Masato Kodama

Abstract—This paper addresses the evaluation of object detection performance for non-contact safety-related sensors in low-visibility environments due to adverse weather conditions. An evaluation metric, MOT (Minimum Object-detectable Transmittance), is proposed to quantitatively evaluate the influence of the low-visibility environments on the object detection performance. Traditionally, the Meteorological Optical Range (MOR) has been used for this purpose. However, MOR is not appropriate for the sensor evaluation because it is a meteorological metric which is optimized for human eyes to estimate the distance at which a person can see clearly through an atmosphere. On the other hand, MOT is a physical and optical measure that quantifies the relationship between the spatial transmittance and the distance at which a sensor can detect a specified object. It is specialized for the sensor evaluation and can express the sensor characteristics in the low-visibility environments at each measurement distance. The usefulness of MOT will be demonstrated by presenting the experimental results of MOT measurements for various sensor devices in a fog space reproduced with environmental simulator equipment.

Index Terms—Performance evaluation, safety-related sensor, object detection, low-visibility environment, spatial transmittance.

Object Detectable: **46.2%** transmittance

Object Distance Measurable: **96.6%** transmittance
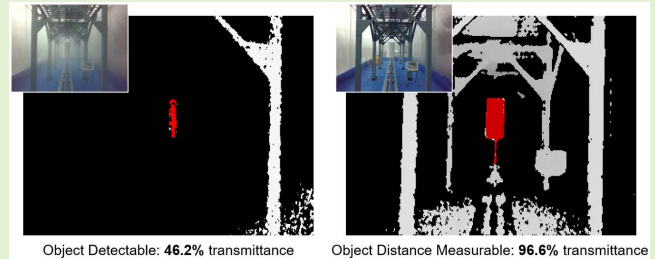
I. INTRODUCTION

BECAUSE of rapid advances in AI technology, autonomous machines in outdoor public spaces are entering the practical application stage, such as autonomous vehicles, automated farm machinery and mobile service robots. Here, the problem is to ensure safety. The machines, if they are to share the space with persons, must have non-contact safety-related sensors to detect approaching the persons and stop themselves safely. Those sensors shall not be degraded in their detection performance under any environmental conditions if they are within their intended use.

In the outdoor environments, light interference from sunlight and the adverse weather conditions, such as rain, snow, and fog, can degrade the detection performance (Fig. 1). There will be a strong demand for sensors that are robust to these external disturbances. This requires two technological developments to be established. One is the core technology

of sensing, which must detect objects even in the presence of the disturbances. The other is an evaluation technology that verifies the object detection performance and guarantees that the sensor function will work reliably whenever it is required.

This paper addresses the latter issue, i.e., the sensor evaluation technology in the low-visibility environments. First, we propose an evaluation metric, MOT (Minimum Object-detectable Transmittance), which is the minimum spatial transmittance at which a sensor can detect a person or a specified object at a specified distance.

The manufacturer of a safety-related sensor is required to provide information on the conditions under which the sensor can reliably detect the specified object as information for use [1]. The low visibility of the atmosphere is one of the important environmental conditions.

Some sensor products based on optical principles have very poor robustness in the low-visibility environments. To ensure that such sensors are not adopted for outdoor safety-related systems, their performance have to be properly evaluated, certificated, and then provided to sensor users.

MOT is a metric for sensor performance in the low-visibility environments; with MOT, it is represented, for example, "The MOT_4 value of this sensor is 0.95 in a fog environment." This means that the sensor can detect objects in fog with a spatial transmittance of 95% at a measurement distance of 4 m.

On the other hand, when using the conventional metric MOR (Meteorological Optical Range), which is commonly

Fig. 1. Robot in an outdoor environment.

used in the meteorological field, it is as "This sensor is available in a fog environment with a MOR of 320 m." The problem is that this representation does not contain any distance-dependent information about object detection, which is mandatory for sensor specifications. Therefore, the sensor users must analyze and test the distance-dependence by themselves. It will require a lot of man-hours and cost.

With MOT, the sensor users can skip them and reduce the total cost of system development. The sensor manufacturers can also reduce their development costs by clarifying the sensor performance to be achieved by new products.

The sensor evaluation by MOT is useful for integrators, who integrate an outdoor safety-related sensor system from multiple different safety-related sensors to achieve redundancy and diversity in sensing, as well as improved sensor performance and limitations in use [1].

In this paper, experimental results are presented to demonstrate the usefulness of MOT. We conducted tests on several different consumer sensors in a fog space reproduced with environmental simulator equipment and obtained measurement results that well represent the characteristics of the sensors. This suggests that MOT can be used universally to evaluate the detection performance of the safety-related sensors.

A. Scope

When discussing the safety requirements and evaluation metrics for machines, it is important to clarify the scope of application [1].

The application of the sensor addressed in this paper is the autonomous machines for outdoor use, such as mobile robots, which are expected to be in great demand in the future. And we deal with the low-visibility environments due to adverse weather conditions, such as rainfall, snowfall and fog, which can affect the detection performance of the sensors and to which they are exposed frequently.

The evaluation target in this paper is a range-imaging sensor device, a so-called "depth camera", intended to be used in safety-related systems. It captures a scene as an RGBD image, i.e., a 2D array that stores the color and distance information of the measurement points corresponding to each pixel. It is often used to measure relatively short distances.

There are three major sensing principles, which are Time-of-Flight (TOF), stereo vision (SV) and structured light (SL). A TOF sensor measures the time it takes for a periodic light beam emitted from an LED or laser to be reflected by a

subject and return to a receiver and estimates the distance to the subject based on the principle of light speed invariance. SV and SL type sensors use the principle of triangulation in multiple-view geometry to measure the distance to the feature point of the subject [3], [4].

At present, there are only a few safety-related depth cameras that are commercially available. However, they will be the mainstream in the safety-related field soon, because they have an extremely large market for applications such as mobile communications and gaming devices, which will undoubtedly become more powerful and less expensive.

The discussion in this paper can be also be applied to LiDAR sensors, since they are essentially based on the same sensing principles as the TOF-based depth cameras. The LiDAR sensors are primarily used for medium- to long-range distance measurement by laser beam single- or multi-planar scanning.

Radar and ultrasound sensors are not treated in this paper because they differ in measurement range and resolution and have different applications. Proximity and contact sensors are not covered in this paper for the same reason.

II. BACKGROUND AND RELATED WORK

A. Standardization

The evaluation technology for the sensor performance in outdoor environments are directly relevant to the international standardization. It is necessary for manufacturers, suppliers, and system integrators for designing safety-related machines and systems to be operated outdoors. In recent years, international standards for new sensor products have been developed. IEC/TS 61496-4-3:2015 [5] and IEC 61496-3:2018 [6] are specified requirements for the stereo-vision-based and the TOF-based safety sensors, respectively. However, these standards are both intended for indoor factory environments.

A new generic standard for safety-related sensors, IEC/TS 62998-1:2019 [1], considers outdoor environments. This standard specifies environmental factors such as temperature, humidity, precipitation, barometric pressure, sunlight, vibration, etc. that must be considered when designing safety sensors.

However, no quantitative values are mentioned for low visibility due to fog and snowfall, it just says "shall be considered."

As described above, in the field of the international standardization, recent advances in the sensor technologies make it necessary to develop the evaluation criteria and test methods for the new sensor devices in outdoor environments. This paper addresses these issues.

B. Meteorology

The meteorological term "visibility" is the maximum distance at which an object can be clearly observed by human eyes, which is an important meteorological measurement for aircraft and ship operations. The mechanical instrumentation of the meteorological visibility is defined by the World Meteorological Organization (WMO) as the Meteorological Optical Range (MOR), which is "the length of path in the atmosphere

required to reduce the luminous flux in a collimated beam from an incandescent lamp, at a colour temperature of 2700 K, to 5% of its original value" [7].

The value of MOR [m] is calculated by applying Eq. (1) based on Koschmieder's law:

$$MOR = x \times \frac{\ln c_0}{\ln T} = -\frac{\ln c_0}{\alpha}, \tag{1}$$

where T is the transmission of atmosphere observed at a distance x [m] from the light source, α is the absorption coefficient of the atmosphere and c_0 is a constant that represents the threshold of the attenuation rate of light. The value of c_0 is empirically set to 0.02 (2%) in most cases, though it is sometimes set to 0.05 (5%), according to the definition of the MOR [8].

MOR, however, is originally a metric for estimating the distance that an airplane or ship's operator can see clearly through the atmosphere, and therefore it may not always be appropriate for the safety-related sensors of the service robots. For example, MOR is:

- Scale mismatch. While the actual range of MOR is commonly measured from a few meters to several kilometers, the detection area of the safety-related sensors for the service robots is at most a few meters to a several dozen meters.
- Distance independence. The evaluation of a sensor should be conducted within the range of measurement distances intended for the sensor. However, MOR is difficult to represent distance-dependent values because it represents the physical properties of the atmosphere itself.
  If a robot is intended to detect a person at 5 m distance, the manufacturer of the robot will want to know the sensor performance at 5m. In such a case, the information "this sensor can be used in an environment with MOR of 100 m." will be of little use.
- Non-linear, as can be seen from Eq. (1). When the measured transmittance exceeds 90%, the MOR value increases rapidly. For example, for a sensor intended to use at around 10 m, there should be little difference between an environment with 94% transmittance and one with 96% transmittance, but the corresponding MOR values are 632 m and 968 m, which is an extremely large difference.
- Optimized for human eyes, as is obvious from its definition. For the sensor evaluation, the metrics should be simply determined as a pure optical and physical measurements.

These problems can be avoided by MOT proposed in this paper, which is a metric for atmospheric visibility specialized for the sensor evaluation.

C. Computer Vision and Robotics

In the field of computer vision and robotics, several sensing and image processing technologies have been researched and developed in rainfall, snowfall, and fog environments.

For example, Charette *et al.* have developed a famous smart headlight. Their system uses a camera to estimate the location of precipitation, i.e., raindrops and snowflakes, in front of a car, and then divides the headlights into smaller pieces with a beam splitter to avoid these particles, thereby preventing the scattering and reflection of the illumination by the particles to improve the driver's visibility [9].

Murase's group has proposed a variety of driver assistance technologies that use cameras and various sensors to accurately detect pedestrians, obstacles, driver status and weather conditions in rainy and foggy environments [10].

Muraji *et al.* have proposed a method to compensate for the effect of fog by using multiple modulation frequencies in distance measurement with a TOF camera [11].

Liu *et al.* have proposed a vision-based system for detecting runways during aircraft approach and landing under low-visibility environments. Instead of using expensive sensors such as millimeter-wave radar, they combine multi-sensor fusion and image processing to achieve a low-cost sensor system [12].

These studies are on fundamental theories and core techniques for improving sensor performance or cost-effectiveness in low-visibility environments, which are extremely important for the practical application of outdoor automated machines.

However, in addition to these state-of-the-art sensing technologies, evaluation technologies are also essential to ensure that safety sensor products work as intended. This paper addresses this issue and attempts to establish criteria for evaluating sensor performance in the low-visibility environments.

D. Our Previous Work

The metric proposed in this paper was inspired by our previous studies on sensor evaluation in outdoor environments.

We have developed artificial sunlight lampheads for a light interference test method [13] and a simulated-snow chamber to reproduce the visibility reduction due to snowfall at room temperature [14]. To investigate the sensor effects of visibility reduction due to fog, basic experiments were conducted, and the results were published [15].

In these studies, however, we had to use MOR as an evaluation metric, despite the problems mentioned above; we believe that MOT can better represent the characteristics of the sensor.

III. MINIMUM OBJECT-DETECTABLE TRANSMITTANCE, MOT

A. Definition

In this section, we provide the definition of Minimum Object-detectable Transmittance, MOT, proposed in this paper. MOT is a metric for evaluating sensor performance on object recognition in low-visibility environments.

A spatial transmittance at an observation distance d in the atmosphere with an absorption coefficient α is determined by Beer-Lambert law,

$$T_d = e^{-\alpha d}. \tag{2}$$

Here, MOT_d is defined as "the minimum transmittance of a space in which a sensor detect a specific object at a distance of d m." It is formulated by the following equation,

$$MOT_d = \min_{\alpha \in A} e^{-\alpha d}, \tag{3}$$

where A is the set of atmospheric conditions under which the sensor detect a test piece. Normally the test piece is a three-dimensional body with a shape, size, and surface reflectivity that is representative of a person or part of a person.

Experimentally, an MOT_d value is determined by choosing the spatial medium with the minimum transmittance from among various media at which the sensor detect the object. So, the min operator in Eq. (3) means to choose the absorption coefficient α of the medium so that the transmittance $T_d = e^{-\alpha d}$ is minimized among all the possible media.

MOT_d values are directly transformed to the corresponding MOR values by Eq. (1). That is, for example,

- "The MOT_4 of this sensor is 80%." and
- "The MOR of the space where this sensor can detect the specified object at 4 meters away is 70 meters."

are mathematically and physically equivalent. On the other hand, MOR values cannot be transformed to the MOT values. It requires additional information about the measurement distance for object detection.

As mentioned in the previous section, MOR is not always appropriate for evaluating the sensor performance. On the other hand, MOT is specified for the sensor evaluation. It has following features.

- Scale and distance dependent: MOT can represent the sensor performance according to the measurement distance, as is obvious from its definition. As described above, MOT and MOR are equivalent mathematically and physically. However, from a practical point of view, MOT is much easier to use. If we try to use MOR forcibly, we have to add extra information about the measurement distance, such as "at distance of 4 m", because it is mandatory for sensor evaluation. And this is not the original usage of MOR, so it may cause confusion to the user.
- Linear: An MOT value is simply measured as spatial transmittance at a distance from the test piece to the sensor. It provides an intuitive understanding of the sensor performance against the atmospheric visibility.

  As described in Clause II.B, the MOR values increase exponentially as the spatial transmittance increases. For example, if two sensors, S1 and S2, have MOT_4 of 90% and 95%, respectively, in fog environments, then they can be adequately represented that their performance is almost the same. Everyone can see that they both failed to detect objects even in a very light fog environment. However, when they are converted to the corresponding MOR values, it results in 148 m for S1 and 383 m for S2. This will give the users the impression that there is a large difference in performance between them.
- Independent of the human eyes: MOT is a simple physical parameter.
- Compatible with MOR: Since MOR is an indispensable metric in the traditional fields, it is important to be able to link MOT with MOR. An MOT value is directly converted to a corresponding MOR value as described above.
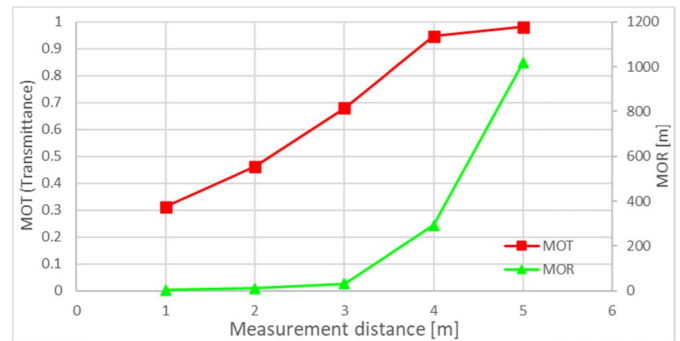

Fig. 2. Comparison of MOT and MOR. This graph is a measurement example that well illustrates the difference between MOT and MOR. The red graph plots the MOT_d values of a certain sensor, and the green one plots the corresponding MOR values converted by Eq. (1). The MOT value adequately represents the sensor performance depending on the measurement distance. On the other hand, it is necessary for MOR to add extra distance-dependent information forcibly. That is, e.g., the MOR value of 4 m means that this sensor can detect a specific object at 4 m apart in a fog with a MOR of 228 m. It is confusing and misleading. Additionally, MOR is nonlinear. The graph shows that, at distances below 3 m, the MOR values do not sufficiently represent the difference in the sensor performance; conversely, at 4 m and 5 m, it appears as if the performance difference is extremely large.

Fig. 2 shows the MOT values of one sensor and their corresponding MOR values for comparison. In this example, the MOT values are increase almost linearly up to 4 m and there is little difference at distances of 4 m and 5 m, both above 0.9 transmittance. Indeed, at such short observation distances, the space with $T_d > 0.9$ is almost clear. On the other hand, the corresponding MOR values increase exponentially, resulting in an extremely large difference between 4 m and 5 m.

B. Two Types of MOT

MOT is classified into two types, MODT (Minimum Object-Detectable Transmittance) and MOMT (Minimum Object-detectable and Measurable Transmittance), according to the object detection states of a sensor. When an object is in the detection zone of the sensor, the sensor can take one of the following three states depending on the spatial transmittance, as shown in Fig. 3.

1. Measurable: When the spatial transmittance is sufficiently high, the sensor can detect the object within its detection zone and measure the distance within the assumed error range, and it can provide normal operation. The minimum transmittance at which the sensor maintains this state is called MOMT.
2. Detectable: As the spatial transmittance decreases, the sensor may not be able to measure the object distance correctly, even if it can detect the object or something within the detection zone. The minimum spatial transmittance at which the sensor maintains this state is called MODT. In this state, the sensor cannot provide the normal operation, but it can stop machines safely to prevent failure to danger. In other words, it works as a safety-related sensor.
3. Undetectable: When the transmittance is further reduced, the sensor becomes unable to detect the object. This results in a failure to danger since the machine cannot be stopped.
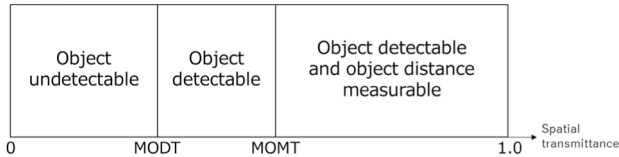
Fig. 3. Relationship between MODT, MOMT and object detection states depending on spatial transmittance.

Fig. 4. The thickest fog environment reproducible with the simulator. The transmittance at 5 m distance is less than 2%, $T_5 \leq 0.02$. The yellow-green spindle in the front top of the image is one of the fog generators. The large pale-green steel frames are parts of a rainfall apparatus, not related to this experiment.

In general, as shown in Fig. 3, it holds that

$$0.0 \leq \text{MODT} \leq \text{MOMT} \leq 1.0. \tag{4}$$

The MOMT and MODT values are expected to be the same or almost the same, but as shown later in the experimental results, they may differ significantly for some sensors.

Note that some sensors may always be in Detectable state in the low-visibility environments. In this case, MODT = 0.0. For example, a TOF sensor may detect a group of fog particles in space as a single wall-like object because of scattering. Such sensor does not become "undetectable" no matter how much the spatial transmittance decreases [15]. In principle, it does not fall into failure to danger against low visibility due to fog, although they do not provide normal operation.

C. Wavelength Dependencies of MOT

For rain or fog, the reduction in transmittance is regarded as constant at all wavelengths of light from near-UV to near-infrared, because it can be approximated by applying Mie scattering or geometric optical approximation (diffraction) [16]. For snow, optical occlusion should be considered. In any case, therefore, wavelength dependence is not significant in the evaluation of optical-based sensors.

If evaluation in mediums such as smoke or oil mist, where the transmittance may be wavelength dependent, then spectral MOT corresponding to the wavelength λ should be used,

$$MOT_d^\lambda = \min_{\alpha_\lambda \in A} e^{-\alpha_\lambda d}. \tag{5}$$

IV. EXPERIMENTAL RESULTS

A. Experiment Environment

In this chapter, we present the experimental results of MOT measurements in a fog environment reproduced with environmental simulator equipment to demonstrate the usefulness of MOT.
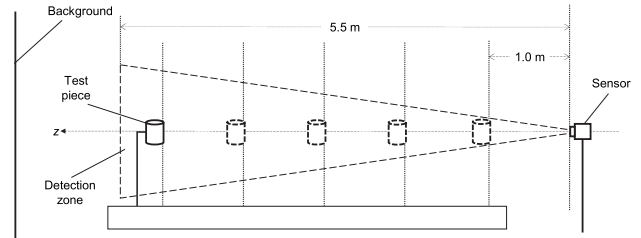

Fig. 5. Experimental setup. The cylindrical test piece was placed at an accurately measured distance from its surface to the sensor optical window. Then the MOT values were measured from 1.0 to 5.0 m at 1.0 m intervals. The detection zone was determined as up to 5.5 m from the sensor. z is the depth along the optical axis in the sensor coordinate system. The background was the semi-transparent plastic screen that surrounds the test space. The illumination was fluorescent, and the illuminance was approximately 240 lx at the bottom of the test piece location.

The simulator equipment has two fog generators (AKIMist E, H.IKEUCHI & Co., Ltd.) and a test space of 3,400 mm width, 7,600 mm depth, and 2,800 mm height, surrounded by semi-transparent plastic screens. The fog generators fill the test space with water mist particles averaging 7 μm in diameter to reproduce a near-natural radiant fog [17]. The thickest fog reproducible with the simulator has less than 2% transmittance at 5 m, $T_5 \leq 0.02$, as shown in Fig. 4. For measuring the transmittance values, we used the spatial spectral transmittance meter which consists of a projector and a receiver placed at both ends of the test space at intervals of 6.71 meters [13], [14].

B. Experimental Setup

Fig. 5 shows the setup of the experiment. For the test piece, a cylinder with 200 mm diameter, 400 mm height, and about 80% surface reflectance was used, which is representative of the torso of an adult. The MOT values were measured from 1.0 to 5.0 m at 1.0 m intervals for the test piece.

The sensor devices tested in this experiment are the following six models of distance-imaging sensor products using different sensing principles described in Clause I.A.

- Sensor A and B (TOF)
- Sensor C and D (SL)
- Sensor E and F (SV)

Note that these sensor products are all for general consumer use, not for safety-related applications. In addition, we did not make any parameter tuning to each sensor in this experiment.

The MOT values of a sensor should be measured according to its own object detection function that any safety-related sensor ought to have. However, the above sensor devices are not safety-related and do not have the function. Therefore, we developed a software module for object detection, emulated SRS, to evaluate the sensor devices under the same conditions.

The emulated SRS module processes a distance image obtained from the sensor and detects connected regions within the detection zone as "objects." See Appendix for more details about emulated SRS.

Fig. 6 shows examples of the object detection with Sensor A. In the object recognition images, pixels far from the sensor are in darker colors and areas detected as the objects are marked in red. Pixels with no distance data are in black. It shows that in the thick fog, Sensor A could not measure
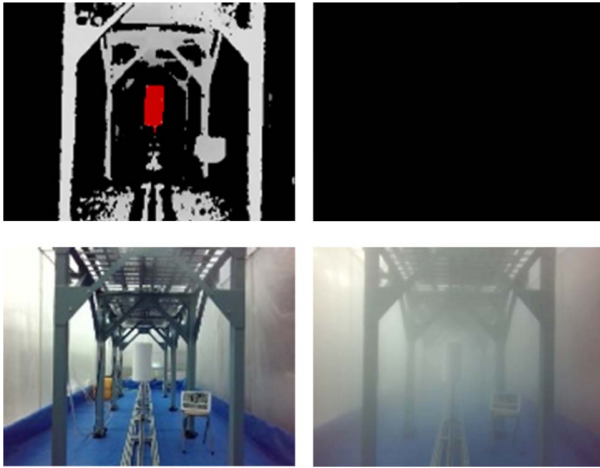
Fig. 6. Examples of distance measurement and object detection. The target sensor was Sensor A and the test piece was placed at 2 m distance from the sensor. The top two images show the object detection results. The left image shows the case without fog, and the right one shows the case with the thickest fog reproducible with the simulator equipment. The bottom two images show the corresponding RGB images for reference.

any distance at all, so the object detection image is all black pixels.

C. MOT Determination Criteria and Experimental Procedure

In this experiment, the determination of whether an object was successfully detected or not was made as follows.

- Detectable: The test piece or something else is continuously detected at the same location within the detection zone. The accuracy of the distance measurement does not matter.
- Measurable: The test piece is continuously detected and the z-coordinate of its center of gravity center is less than $\pm 10\%$ of the ground truth.

To achieve measurements in as uniform a fog environment as possible, the experiment was carried out as following steps.

1. First, fill the test space with the thickest fog possible with the equipment, and stop the fog generation.
2. Measure the spatial transmittance continuously and execute the object detection simultaneously while the fog gradually clears.
3. Record the transmittance at the time determined to be Detectable and Measurable according to the above criteria as MODT and MOMT, respectively.

As an example, the MOT measurement result is shown in Fig. 7. In this case, the test piece was detected at a time of about 155 seconds, so the corresponding MODT was 0.46. However, at that time, the object distance was wrongly measured to be about 0.3 m. Then, at about 467 seconds, the measurement was successful (assumed to be 2 m $\pm$ 10%), so the corresponding MOMT was 0.97.

D. Measurement Results and Discussion

As a result of the experiment, the MOT of some sensors did not change significantly regardless of the distance. Fig. 8 shows the results of MOT measurements for Sensors B, C, D,
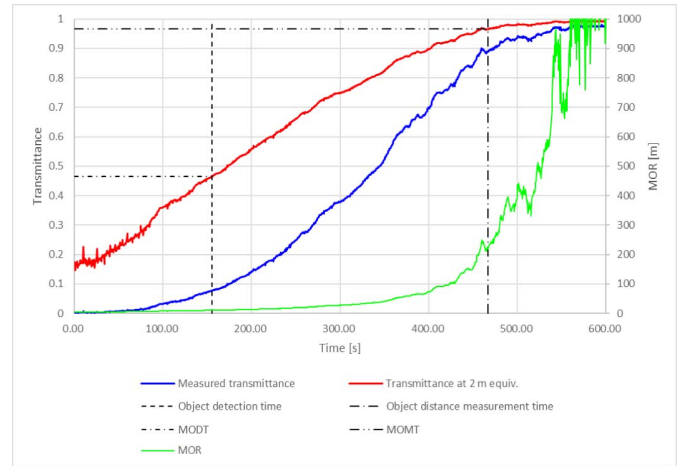

Fig. 7. Example of MOT measurements. The target sensor was Sensor A, and the measurement distance was 2 m. The graph shows the transmittance T measured with the transmittance meter, and T_2 converted to the transmittance at 2 m. For comparison, the MOR values converted from T are also shown. The graphs plot the time series data obtained in an MOT measurement experiment, and it follows the execution process of the three steps to measure the MOT described in Clause IV.C. Each of the steps corresponds to the following times on the time axis.
- 0 s: Filled the test space with the thickest fog (step 1)
- 0 to 470 s: Measured the spatial transmittance and executed the object detection continuously while the fog gradually cleared (step 2)
- 160 s: Detected the test piece and recorded the value of MODT (step 3)
- 470 s: Measured the distance to the test piece correctly and recorded the value of MOMT (step 3).

and E from 1 to 5 m. For these sensors, there was no distinction between MODT and MOMT because object detection and distance measurement were successfully achieved with the same transmittances, that is, when an object was detected, the measurement accuracy was also within the error range.

The graph shows that the MOT values tend to increase slightly with distance, or do not change significantly. This result suggests that for a certain type of sensors, their MOT values are always almost constant regardless of the measurement distance.

However, there are exceptions. For some sensors, the MOT values varied significantly depending on the distance and MODT and MOMT had to be determined separately. Such examples for Sensor A (TOF) and Sensor F (SV) are shown in Fig. 9. The data of Sensor A at 2 m are identical to those in Fig. 7.

The result of Sensor A was unique: the MOMT values were almost constant regardless of the measurement distance, like the sensors in Fig. 8. On the other hand, the MODT values were almost 0.5 up to 3 m, which were quite different from the MOMT values. The wrong measurement distances were 0.3 m, which is consistent with the minimum measurement distance of this sensor.

For Sensor F, as shown in the example of detection results in the lower right of Fig. 9, it always detected a wall-like object in the entire field of view under fog conditions, without parameter tuning. This is like the behavior observed with the TOF sensors in our previous report [15]. So, the MODT values of Sensor F are meaningless because they are consistent with the transmittance of the thickest fog with the simulator.
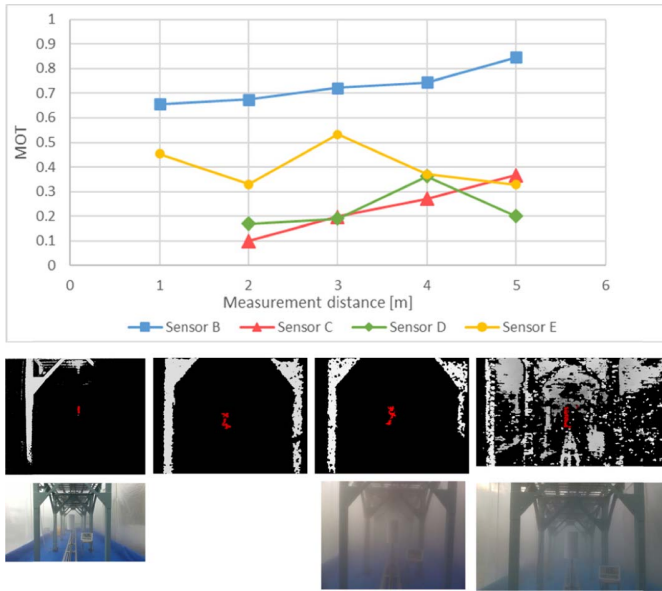
Fig. 8. MOT measurement results for Sensors B (TOF), C, D (SL), and E (SV). The images at the middle show the object detection results of each sensor at MOT with a distance of 2 m. The bottom images show the corresponding RGB images for reference, except for sensor C, which does not provide an RGB image. For these sensors, MOT is used because there was no distinction between MODT and MOMT. For Sensors C and D, the MOT_1 values are omitted, because these sensors were able to detect the test piece at 1 m distance even in the thickest fog with the simulator, and the MOT_1 values could not be determined.
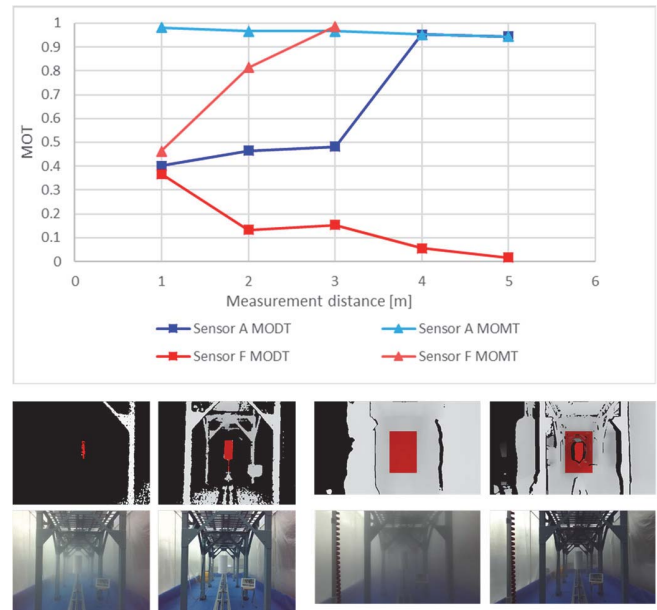

Fig. 9. MOT measurement results for Sensors A (TOF) and F (SV). The images at the middle are examples of detection results at 2 m. The two images on the left are the results corresponding to MODT and MOMT of Sensor A, which are identical to the images in Fig. 7, and the two images on the right are corresponding to those of Sensor F. The bottom images show the corresponding RGB images for reference. For these sensors, MODT and MOMT have to be distinguished because the distance measurements were wrong at the transmittance where the object could be detected. The graph shows that the measured MODT and MODT values varied significantly depending on the distance. For Sensor F, the values of MOT_4 and MOT_5 are omitted, because the sensor could not separate the object from the background to detect it at 4 and 5 m due to the similarity of their colors. Note that this result can be due to the absence of any parameter tuning of the sensor.

Theoretically, they are equal to the smallest real value above zero. As mentioned in Clause III.B, this type of sensors, which detect the wall-like object in low-visibility environments, result in a safety-side failure.

As described above, by using MOT, we were able to describe the characteristics of the sensors in low-visibility environments in an intuitive and easy-to-understand manner.

Additionally, the following knowledge was obtained in this experiment.

- The performance of TOF sensors (sensors A and B) in object detection and distance measurement is significantly affected by fog. This reinforces the results of our previous paper [15].
- In the previous experiment [15], the TOF sensors showed the characteristics of detecting a wall-like object in the entire field of view, like Sensor F in Fig. 9. We assumed that this occurred because the light scattered by the fog particles was regarded as the light reflected from a single large object. However, in this experiment, no such behavior was observed for the tested TOF sensors (Sensors A and B). The sensors tested in the previous experiment were early models for TOF sensors. So their internal processing algorithms may have been naïve compared to those of resent models that can eliminate the effects of the scattered light.
- The SV sensors (Sensor E and F) can be generally more robust to the fog environments than the TOF sensors. However, their characteristics can vary widely from product to product. They are highly dependent on the stereo-correspondence-search algorithms, which can be freely designed according to their purpose. If the algorithm

tries to reconstruct a smoothly connected 3D surface, as probably Sensor F does, it will not perform well in a blurry environment such as fog.
- The SL sensors (Sensors C and D) are robust to the fog environments. The object detection and measurement functions worked effectively even in dense fog with a transmittance T_d of almost 0.3 or less. At a short distance of 1 m, these sensors were able to detect the test piece even in the thickest fog reproducible with the simulator, and thus the MOT_1 values could not be determined, as shown in Fig. 8. The results of the previous experiment showed a similar tendency. We think that the active projection of the structured light can contribute to the robustness.
- For scattering of light due to the size of the fog particles, Mie scattering is applied within the wavelength range of visible to near-infrared light [16], so that the decrease in transmittance in the fog environment is independent of wavelength. This has been verified by the experimental results in our previous paper [15]. Therefore, in the experiments presented in this paper, we did not consider wavelength because we tested sensors that use the visible or near-infrared light.

If the sensor performance depends on the wavelength, the analyses and experiments must be based on Eq. (5). For example, for particles smaller than fog, since
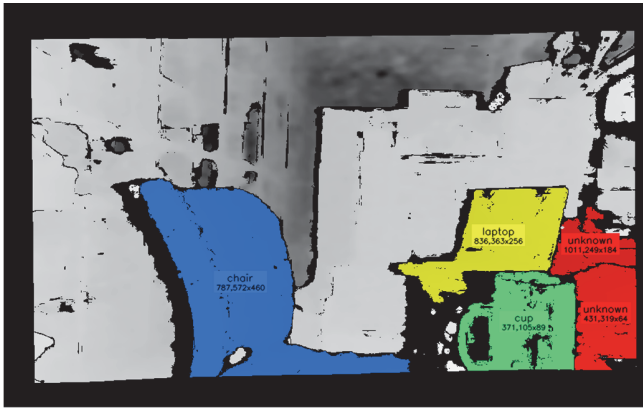
Fig. 10. Example of object detection results by the emulated SRS module. The intensity of the pixels represents the distance, with the darker pixels representing the farther distance. Black reasons represent missing data. The black frame on the outer edges is due to the rectification process on the input range image [23]. The detected object regions are marked in color. The digits in the region are the average distance from the sensor and the width and the height of the region in millimeters. The labels of each region (person, chair, etc.) indicate the classification results using the Deep Learning technology [22].
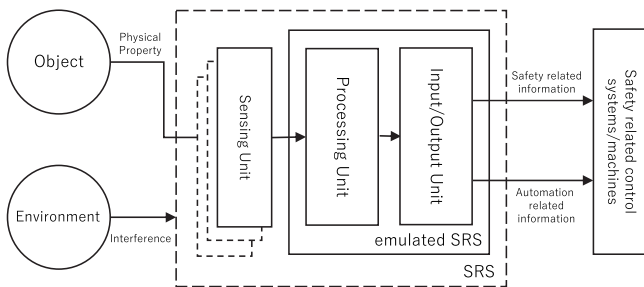

Fig. 11. Architecture of emulated SRS. The emulated SRS module implements the processing unit and the input/output unit among the three units according to IEC/TS 62998-1 that specifies the requirements of the Safety-Related Sensor (SRS).

Rayleigh scattering is applied instead of Mie scattering, the transmittance depends on the wavelength.

V. CONCLUSION

This paper proposed MOT as one of the criteria for evaluating the object detection performance of non-contact optical safety-related sensors in low-visibility environments. MOT is a metric for quantitatively evaluating the effect of visibility reduction on the sensor performance depending on the measurement distances. The experimental results show that it is useful to express the sensor characteristics.

Our future task is to statistically verify the relationship between the sensor performance and MOT. In this presented experiment, the distance-independence of MOT was observed in four out of the six sensors tested. This suggests the hypothesis that the detection performance of a sensor is determined by the amount of light attenuation. We will verify this hypothesis by accumulating more experimental data.

The MOT values of a sensor product should be provided to sensor users and sensor-system integrators as information for use. They will help select the appropriate safety-related sensor products for designing application systems in outdoor. We hope that MOT will lead to the widespread use of outdoor safety-related sensors and to further improvements in the safety of outdoor machinery.
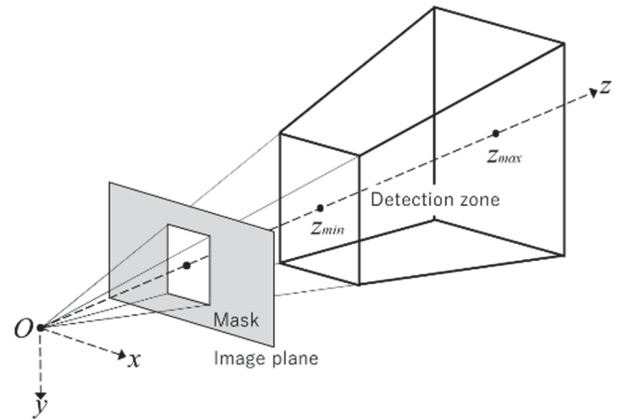

Fig. 12. Geometry of emulated SRS. The detection zone is a frustum determined by the masking process and the two parameters, z_{min} and z_{max} on the optical axis of the sensor.

APPENDIX
OBJECT DETECTION ALGORITHM AND ITS IMPLEMENTATION

We have developed a software module, emulated SRS, emulated Safety-Related Sensor, that can be commonly used for object detection in evaluating different range-imaging sensor devices.

The emulated SRS module, previously called experimental or emulated VBPD [13], [15], unifies the interface of the sensor devices, executes object detection by using a common "mature" algorithm, and visualizes/outputs the results of the range-imaging and the object detection. Fig. 10 shows an example of object detection results with the emulated SRS module.

The emulated SRS module is implemented as a ROS package [18]. The latest version is available online [19]. Note that it is just an experimentally emulated implementation of Safety-Related Sensor according to IEC/TS 62998-1, so it does not support the software functional safety [20].

The architecture of the emulated SRS is shown in Fig. 11. It processes an input range-image to detect specified objects within a specified detection zone and outputs detection results as safety-related information. Since the sensing unit is interchangeable, different distance-imaging sensors can be tested and compared with the same detection algorithm.

Fig. 12 shows the geometry of the emulated SRS module. For simplicity, the detection zone is a frustum determined by the masking process on the image plane and the two parameters, z_{min} and z_{max}, on the optical axis of the sensor.

The object detection algorithm in the emulated SRS is based on the traditional Connected-Component Labeling (CCL) [21], which is found in image processing textbooks. Therefore, we believe that this algorithm is mature enough and can be commonly and fundamentally used for sensor evaluation.

The algorithm is described step by step as follows:

0. The data from the sensing unit is a distance image where each pixel has a positive distance value z_{ij}. If no distance value can be measured, the pixel has a negative value.
1. Perform the masking process in Fig. 12. The masked pixels are overwritten with the negative value.

2. Overwrite pixels below z_{min} and above z_{max} with the negative value.

3. Overwrite pixels an 8-neighbour(s) of pixel value greater than or equal to the threshold Δz with the negative value, which are regarded as occluding boundaries. The overwritten pixel values are preserved.

4. Execute the CCL process by treating the image as a binary image with positive pixels as 1 and negative pixels as 0.

5. Restore the occluding boundaries. If the labeled region is surrounded by the occlusion boundaries, integrate it into its own region.

6. Remove regions of size below the threshold S_{min} (pixel or mm^2). These are regarded as noise or non-safety-related objects, i.e., small objects that are not persons or the hazardous objects.

7. Output the safety-related information. A hazardous status is issued if the number of remaining regions, which are regarded as the safety-related objects, is greater than or equal to one. The dimensions of each of the regions are also reported.

8. Execute object classification by the Deep Learning technology [22]. It is beyond the scope of this paper, so we will omit the details.

In all the experiments provided in this paper, the parameters were set to z_{min}: 0 mm, z_{max}: 5500 mm, Δz: 100 mm, and S_{min} : 200 pixels.

References

[1] *Safety of Machinery—Safety-Related Sensors Used for the Protection of Persons*, Standard IEC TS 62998-1, 2019.

[2] *ISO/IE C Directives, Part 2*, ISO/IEC, Geneva, Switzerland, 2016.

[3] R. Hartley and A. Zisserman, *Multiple View Geometry in Computer Vision*. Cambridge, U.K.: Cambridge Univ. Press, 2000.

[4] Y. Shirai, "Recognition of polyhedrons with a range finder," *Pattern Recognit.*, vol. 4, pp. 243–250, Oct. 1972, doi: 10.1016/0031-3203(72)90003-9.

[5] *Safety of Machinery—Electro-Sensitive Protective Equipment—Part 4–3: Particular Requirements for Equipment Using Vision Based Protective Devices (VBPD)—Additional Requirements When Using Stereo Vision Techniques (VBPDST)*, Standard IEC TS 61496-4-3, 2015.

[6] *Safety of Machinery—Electro-Sensitive Protective Equipment—Part 3: Particular Requirements for Active Opto-Electronic Protective Devices Responsive to Diffuse Reflection (AOPDDR)*, Standard IEC 61496-3, 2018.

[7] WMO. (2018). *Guide to Instruments and Methods of Observation Edition 2018*. [Online]. Available: https://library.wmo.int/index.php?id=12407&lvl=notice_display

[8] H. Horvath, "On the applicability of the Koschmieder visibility formula," *Atmos. Environ.*, vol. 5, no. 3, pp. 177–184, 1971, doi: 10.1016/0004-6981(71)90081-3.

[9] R. de Charette, R. Tamburo, P. C. Barnum, A. Rowe, T. Kanade, and S. G. Narasimhan, "Fast reactive control for illumination through rain and snow," in *Proc. IEEE Int. Conf. Comput. Photogr. (ICCP)*, Seattle, WA, USA, Apr. 2012, pp. 1–10, doi: 10.1109/ICCPhot.2012.6215217.

[10] H. Murase, "Image recognition for driver assistance in intelligent vehicles," in *Proc. 15th IAPR Int. Conf. Mach. Vis. Appl. (MVA)*. Nagoya, Japan: Nagoya Univ., 2017, pp. 406–411, doi: 10.23919/MVA.2017.7986887.

[11] T. Muraji, K. Tanaka, T. Funatomi, and Y. Mukaigawa, "Depth from phasor distortions in fog," *Opt. Exp.*, vol. 27, no. 13, pp. 18858–18868, 2019, doi: 10.1364/OE.27.018858.

[12] C. Liu, Q. Zhao, Y. Zhang, and K. Tan, "Runway extraction in low visibility conditions based on sensor fusion method," *IEEE Sensors J.*, vol. 14, no. 6, pp. 1980–1987, Jun. 2014, doi: 10.1109/JSEN.2014.2306911.

[13] Y. Sumi, B. K. Kim, Y. Matsumoto, E. Horiuchi, O. Matsumoto, and K. Ohba, "Outdoor environment simulators for vision-based safety sensors—Artificial sunlight lampheads and simulated-snow chamber," in *Proc. IEEE Workshop Adv. Robot. Social Impacts (ARSO)*, Tokyo, Japan, Nov. 2013, pp. 125–130, doi: 10.1109/ARSO.2013.6705517.

[14] B. K. Kim, Y. Sumi, R. Sagawa, K. Kosugi, and S. Mochizuki, "Visibility reduction based performance evaluation of vision-based safety sensors," in *Proc. IEEE/RSJ Int. Conf. Intell. Robots Syst. (IROS)*, Hamburg, Germany, Sep. 2015, pp. 4692–4697, doi: 10.1109/IROS.2015.7354045.

[15] B. K. Kim and Y. Sumi, "Vision-based safety-related sensors in low visibility by fog," *Sensors*, vol. 20, no. 10, p. 2812, May 2020, doi: 10.3390/s20102812.

[16] H. C. van de Hulst, "Rigorous scattering theory for spheres of arbitrary size (Mie theory)," in *Light Scattering by Small Particles*. New York, NY, USA: Dover, 1981.

[17] R. Tardif and R. M. Rasmussen, "Event-based climatology and typology of fog in the New York City region," *J. Appl. Meteorol. Climatol.*, vol. 46, no. 8, pp. 1141–1168, Aug. 2007, doi: 10.1175/JAM2516.1.

[18] M. Quigley *et al.*, "ROS: An open-source robot operating system," in *Proc. ICRA Workshop Open Source Softw.*, Kobe, Japan, 2009, pp. 1–6

[19] *A ROS Package for Obstacle Detection*. Accessed: Mar. 19, 2021. [Online]. Available: https://github.com/yssmii/emulated_srs

[20] *Functional Safety of Electrical/Electronic/Programmable Electronic Safety-Related Systems—Part 3: Software Requirements*, Standard IEC 61508-3, 2010.

[21] A. Rosenfeld and J. L. Pfaltz, "Sequential operations in digital picture processing," *J. ACM*, vol. 13, no. 4, pp. 471–494, Oct. 1966, doi: 10.1145/321356.321357.

[22] J. Redmon and A. Farhadi, "YOLOv3: An incremental improvement," 2018, *arXiv:1804.02767*. [Online]. Available: http://arxiv.org/abs/1804.02767

[23] D. A. Forsyth and J. Ponce, "Stereopsis," in *Computer Vision: A Modern Approach*, 2nd ed. London, U.K.: Pearson, 2011.

Yasushi Sumi received the Ph.D. degree in engineering from the University of Tsukuba, Japan, in 1993.

He was a Research Scientist with the Electrotechnical Laboratory (ETL), Japan, from 1993 to 1997, and a Senior Research Scientist with ETL from 1997. He was a Visiting Researcher with VTT, Finland, in 2004. He has been a Senior Researcher with National Institute of Advanced Industrial Science and Technology (AIST), Tsukuba, Japan, since 2001. He is an Expert in IEC TC44. He is also working on the international standardization of safety-related sensors. His research interests include robotics, computer vision, and safety systems.

Dr. Sumi was a recipient of the IEEE/RSJ International Conference on Intelligent Robots and Systems (IROS) Best Paper Award in 2011.

Bong Keun Kim received the Ph.D. degree in mechanical engineering from the Pohang University of Science and Technology (POSTECH), Pohang, South Korea, in 2001.

From 2001 to 2002, he was a Postdoctoral Fellow with the Automation Research Center, POSTECH. From 2002 to 2003, he was a Postdoctoral Fellow with the Department of Mechanical Engineering, University of California, Berkeley. From 2003 to 2005, he was a JSPS Postdoctoral Fellow with the Intelligent Systems Research Institute, National Institute of Advanced Industrial Science and Technology (AIST), Tsukuba, Japan. Since 2005, he has been a Senior Researcher with the Dependable Systems Research Team, Industrial Cyber-Physical Systems Research Center, AIST. His research interests include design and control of mechanical systems, robotics and robot applications, and AI applications.

Masato Kodama was born in Kawagoe, Saitama, Japan, in 1977. He received the bachelor's degree in engineering from the Chiba Institute of Technology in 2001. In 2001, he joined Altech Corporation. He has participated in various development projects at Japanese companies. He is currently working on various research projects at National Institute of Advanced Industrial Science and Technology (AIST). His research interests include embedded software, electrical and electronic circuits, and production systems.